Polarization Signatures of Strong Gravity in Black-hole Accretion Discs

Vladimír Karas
Astronomical Institute, Academy of Sciences, Prague, Czech Republic and
Charles University, Faculty of Mathematics and Physics, Prague, Czech Republic
Michal Dovčiak
Astronomical Institute, Academy of Sciences, Prague, Czech Republic
Giorgio Matt
Dipartimento di Fisica, Università degli Studi "Roma Tre", Rome, Italy

We discuss the effects of strong gravity on the polarization properties of a black hole accretion disc. The intrinsic polarization is computed taking into account light scattered on the disc surface and using different approximations. The gravitational field of a black hole influences the Stokes parameters of reflected radiation propagating to a distant observer. The lamp-post model is explored as an example of a specific geometrical arrangement relevant for AGNs. The degree and the angle of polarization are computed as functions of the observer inclination angle, of the inner radius of the disc emitting region, and of other parameters of the model. The expected polarization should be detectable by new generation polarimeters.

1. INTRODUCTION

Accretion discs in central regions of active galactic nuclei are subject to strong external illumination originating from some kind of corona and giving rise to specific spectral features in the X-ray band. In particular, the K-shell lines of iron are found to be prominent around 6–7 keV. It has been shown that the shape of the intrinsic spectra must be further modified by the strong gravitational field of the central mass, and so X-ray spectroscopy could allow us to explore the innermost regions of accretion flows near supermassive black holes [10, 21]. Similar mechanisms operate also in some Galactic black-hole candidates.

Recent *XMM-Newton* observations indicate the rather surprising result that relativistic iron lines are not as common as previously believed; see Bianchi et al. [3] and Yaqoob et al. [24] fort further references. This does not necessarily mean that the iron line is not produced in the innermost regions of accretion discs but the situation is likely to be more complex than in simple, steady scenarios. Some evidence for the line emission arising from orbiting spots is present in the time-resolved spectra of a few AGNs [9]. Even when clearly observed, relativistic lines behave differently than expected. The best example is the puzzling lack of correlation between the line and continuum emission in MCG–6-30-15 [11], unexpected because the very broad line profile clearly indicates that the line originates in the innermost regions of the accretion disc, hence very close to the illuminating source. Miniutti et al. [15] have proposed a solution to this problem in terms of an illuminating source moving along the black-hole rotation axis or very close to it.

Polarimetric studies along with time-resolved spectroscopy could provide additional information about accretion discs in the strong gravity regime, and this may be essential to discriminate between different possible geometries of the source. The idea of using polarimetry to gain additional information about accreting compact objects is not a new one.

In this context it was proposed by Rees [20] that polarized X-rays are of high relevance. Pozdnyakov et al. [19] studied spectral profiles of iron X-ray lines that result from multiple Compton scattering. Various influences affecting polarization (due to magnetic fields, absorption as well as strong gravity) were examined for black-hole accretion discs [1]. Temporal variations of polarization were also discussed, in particular the case of orbiting spots near a black hole [2, 4]. Furthermore, within general relativity framework the polarization has been studied by various authors: see Portsmouth & Bertschinger [18] for a very recent discussion. With the promise of new polarimetric detectors [5], quantitative examination of specific models becomes timely.

2. THE MODEL AND COMPUTATIONS

We have developed a new code for time-dependent analysis of relativistic spectral features originating in black-hole accretion discs [7–9]. Detailed tracking of time-dependent spectral features (time-scale of several kiloseconds) would be particularly relevant for the modelling and interpretation of variable X-ray features. These have been reported in a growing number of active galactic nuclei and tentatively interpreted in terms of reflection iron lines due to flares and spots [7, 12, 22–24]. Narrow fluctuating profiles are often redshifted with respect to the rest energy and they may provide a powerful tool to measure the mass of central black holes in AGNs and Galactic black hole candidates [6, 16].

Since the reflecting medium has a disc-like geometry, a substantial amount of linear polarization is expected in the resulting spectrum because of Compton scattering. Polarization properties of the disc

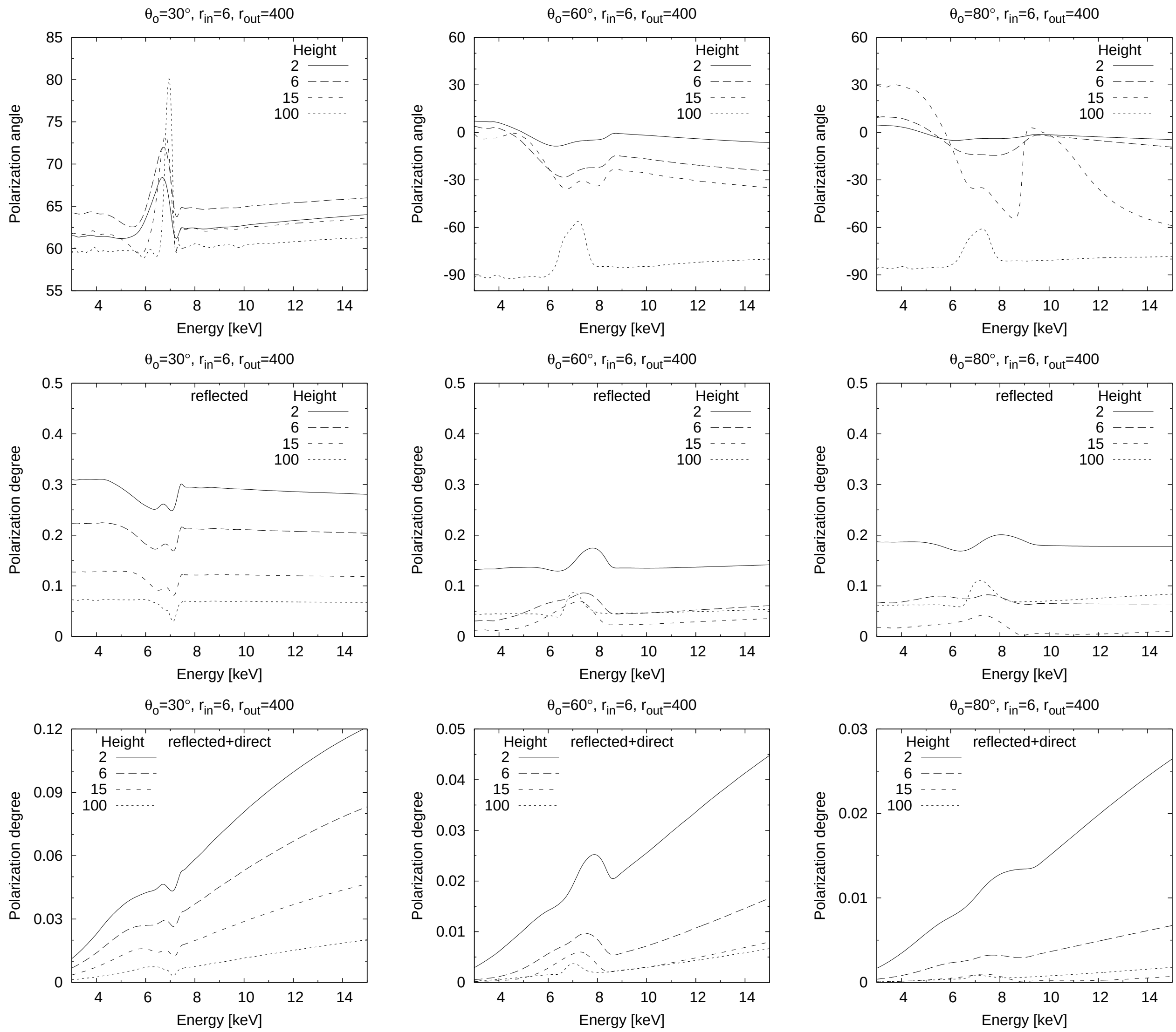

Figure 1: The energy dependence of polarization angle (top panels) and polarization degree (middle panels) due to reflected radiation for different observer's inclination angles ($\theta_{\rm o} = 30°$, $60°$ and $80°$) and for different heights of the primary source ($h = 2$, 6, 15 and 100). Polarization degree for reflected plus direct radiation is also plotted (bottom panels). The emission comes from a disc within $r_{\rm in} = 6$ and $r_{\rm out} = 400$. Isotropic primary radiation with photon index $\Gamma = 2$ and angular momentum of the central black hole $a = 0.9987$ were assumed.

emission are modified by the photon propagation in a gravitational field, providing additional information on its structure. Here we calculate the observed polarization of the reflected radiation assuming the lamppost model for the stationary power-law illuminating source [14, 17]. We assumed a rotating (Kerr) black hole as the only source of the gravitational field, having a common symmetry axis with an accretion disc. The disc was also assumed to be stationary and we restricted ourselves to the time-averaged analysis (we assumed processes that vary at a much slower pace than the light-crossing time at the corresponding radius). The intrinsic polarization of emerging light was computed locally, assuming a plane-parallel scattering layer which was illuminated by light radiated from the primary source.

3. RESULTS

The reflection component has been computed by a Monte-Carlo code. The number of reflected photons is proportional to the incident flux $N_{\rm i}^{S}(E_{\rm p})$ arriving from the primary source,

$$N_{\rm i}^{S}(E_{\rm i}) = N_{\rm p}^{\Omega}(E_{\rm p})\frac{{\rm d}\Omega_{\rm p}}{{\rm d}S_{\rm loc}}\,, \qquad (1)$$

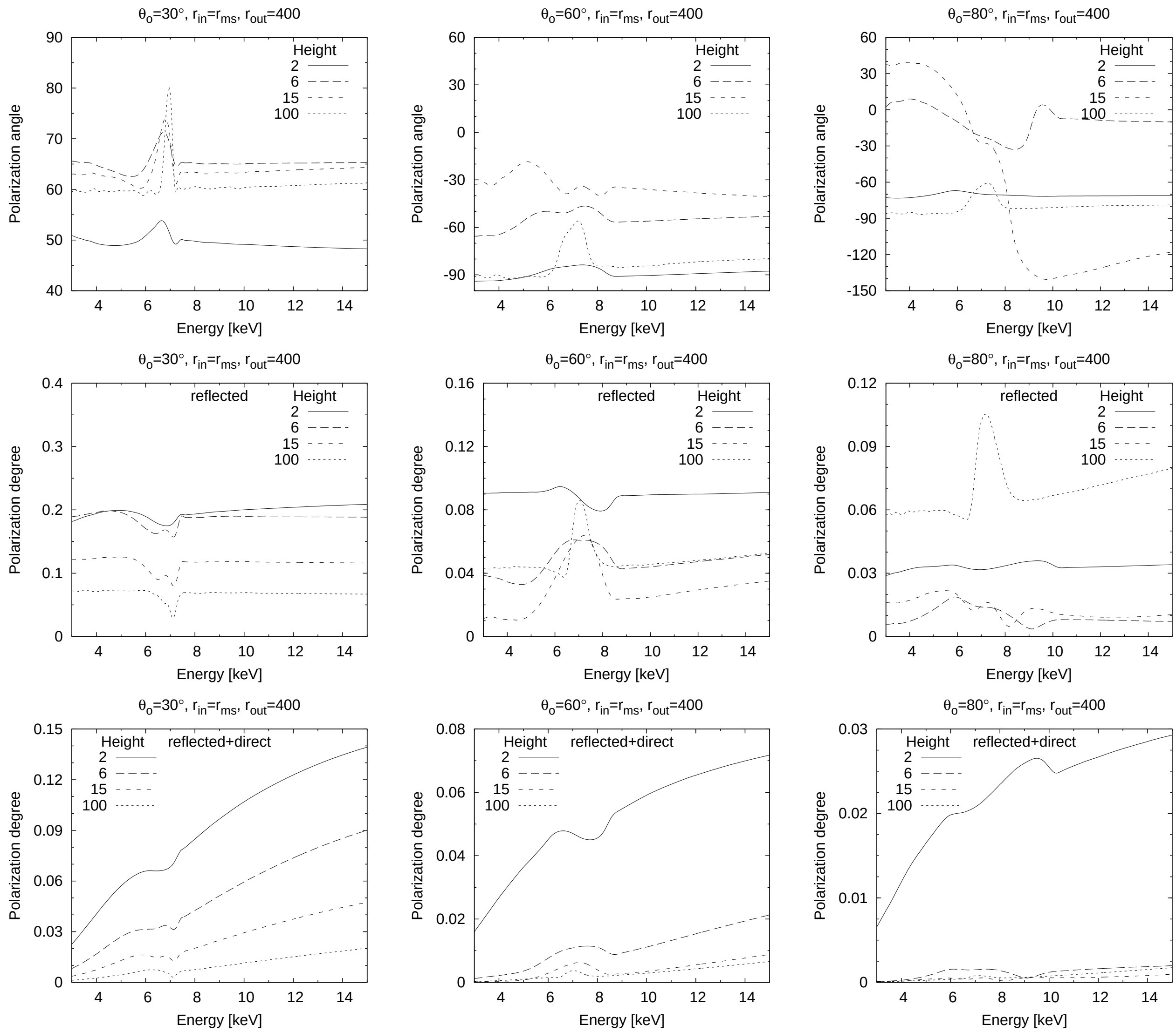

Figure 2: Same as in the previous figure but for disc starting at $r_{\rm in} = 1.20$.

where $N_{\rm p}^{\Omega}(E_{\rm p}) = N_{0\rm p}\, E_{\rm p}^{-\Gamma}$ represents an isotropic and steady power-law primary emission that is emitted into the solid angle $\mathrm{d}\Omega_{\rm p}$ and eventually illuminates the local area element $\mathrm{d}S_{\rm loc}$ on the disc (see refs. [7–9] for a more detailed description of computations and for notation). Four Stokes parameters, I_ν, Q_ν, U_ν and V_ν, entirely describe polarization properties of the scattered light. One has to distinguish the quantities that are determined locally at the point of emission on the disc surface (index 'loc') and those relevant to a distant observer ('o'). We introduce specific Stokes parameters,

$$i_\nu \equiv \frac{I_\nu}{E}\,, \quad q_\nu \equiv \frac{Q_\nu}{E}\,, \quad u_\nu \equiv \frac{U_\nu}{E}\,, \quad v_\nu \equiv \frac{V_\nu}{E}\,, \qquad (2)$$

and then specific Stokes parameters per energy bin, i.e. $\Delta i_{\rm o}$, $\Delta q_{\rm o}$, $\Delta u_{\rm o}$ and $\Delta v_{\rm o}$. The latter quantities are directly measurable, specifying the fluxes of photons with a given polarization. One can write

$$\Delta i_{\rm o}(E,\Delta E) \;=\; N_0 \int \mathrm{d}S \int \mathrm{d}E_{\rm loc}\, i_{\rm loc}(E_{\rm loc})\, F\,, \qquad (3)$$

$$\Delta q_{\rm o}(E,\Delta E) \;=\; N_0 \int \mathrm{d}S \int \mathrm{d}E_{\rm loc} \Big[q_{\rm loc}(E_{\rm loc}) \cos 2\Psi - u_{\rm loc}(E_{\rm loc}) \sin 2\Psi\Big]\, F\,, \qquad (4)$$

$$\Delta u_{\rm o}(E,\Delta E) \;=\; N_0 \int \mathrm{d}S \int \mathrm{d}E_{\rm loc} \Big[q_{\rm loc}(E_{\rm loc}) \sin 2\Psi + u_{\rm loc}(E_{\rm loc}) \cos 2\Psi\Big]\, F\,, \qquad (5)$$

$$\Delta v_{\rm o}(E,\Delta E) \;=\; N_0 \int \mathrm{d}S \int \mathrm{d}E_{\rm loc}\, v_{\rm loc}(E_{\rm loc})\, F\,, \qquad (6)$$

where $F \equiv F(r,\varphi) = g^2\, l\, \mu_{\rm e}\, r$ is the transfer function, g being the total energy shift between observed and emitted photons, l the lensing effect, $\mu_{\rm e}$ the cosine of

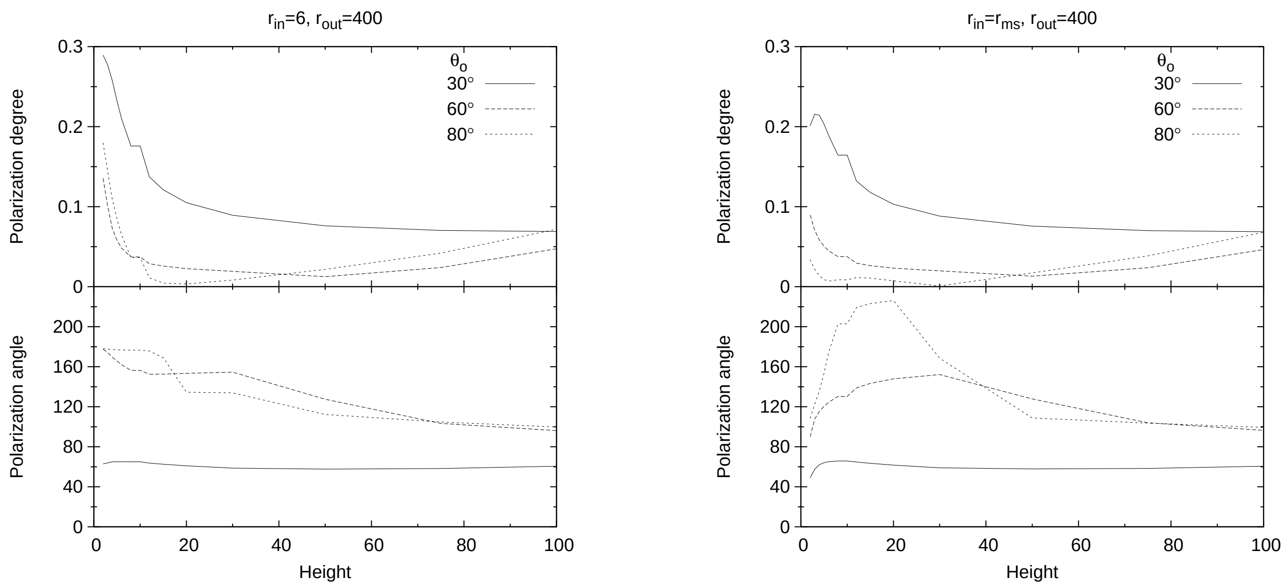

Figure 3: Polarization degree and angle due to reflected radiation integrated over the whole surface of the disc and propagated to the point of observation. Dependence on height h is plotted. Left panel: $r_{\rm in} = 6$; right panel: $r_{\rm in} = 1.20$. In both the panels the energy range was assumed $9 - 12$ keV, the photon index of incident radiation $\Gamma = 2$, the angular momentum $a = 0.9987$.

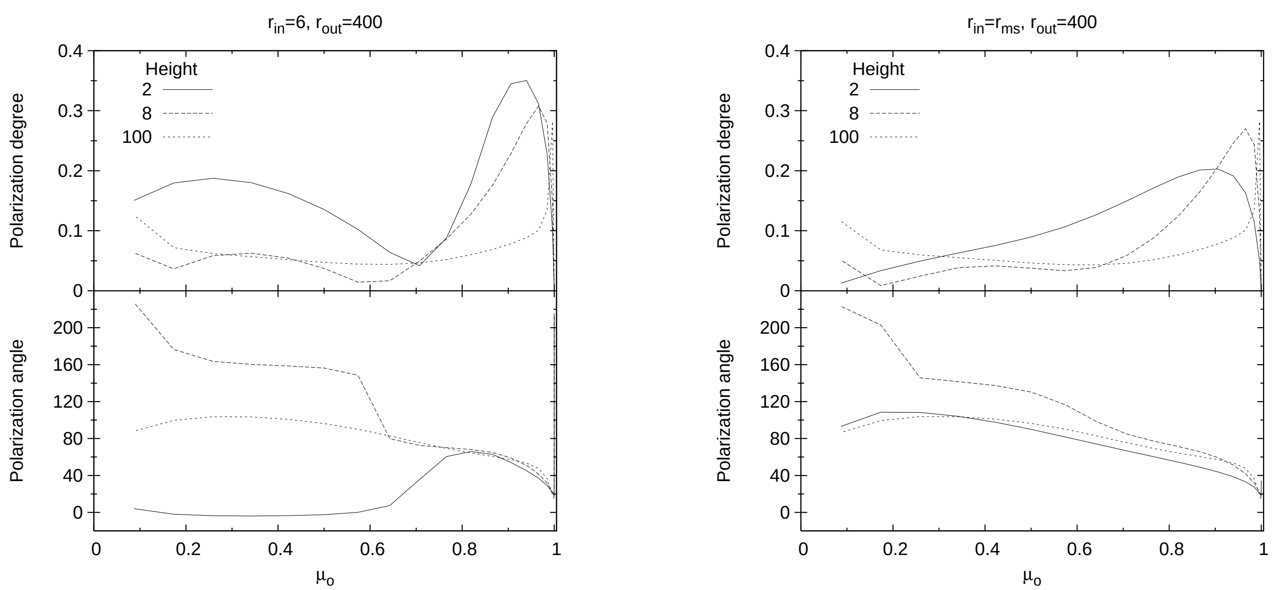

Figure 4: Polarization degree and angle as functions of $\mu_{\rm o}$ (cosine of observer inclination, $\mu_{\rm o} = 0$ corresponds to the edge-on view of the disc). The same model is shown as in the previous figure.

the emission angle, and Ψ the angle by which a vector rotates while it is parallelly transported along the light geodesic.

In Figures 1 and 2 we show, respectively, the energy dependence of polarization angle and polarization degree due to reflected and reflected plus direct radiation. One can see that the polarization of reflected radiation can be as high as thirty percent for small inclinations and small heights of the primary source. Polarization of the reflected radiation depends only weakly on energy, except for the region close to the iron edge at $\sim 7.2\,$keV. In order to compute observable characteristics one has to combine the primary power-law continuum with the reflected component. The polarization degree of the resulting signal depends on the ratio between the two components and also on

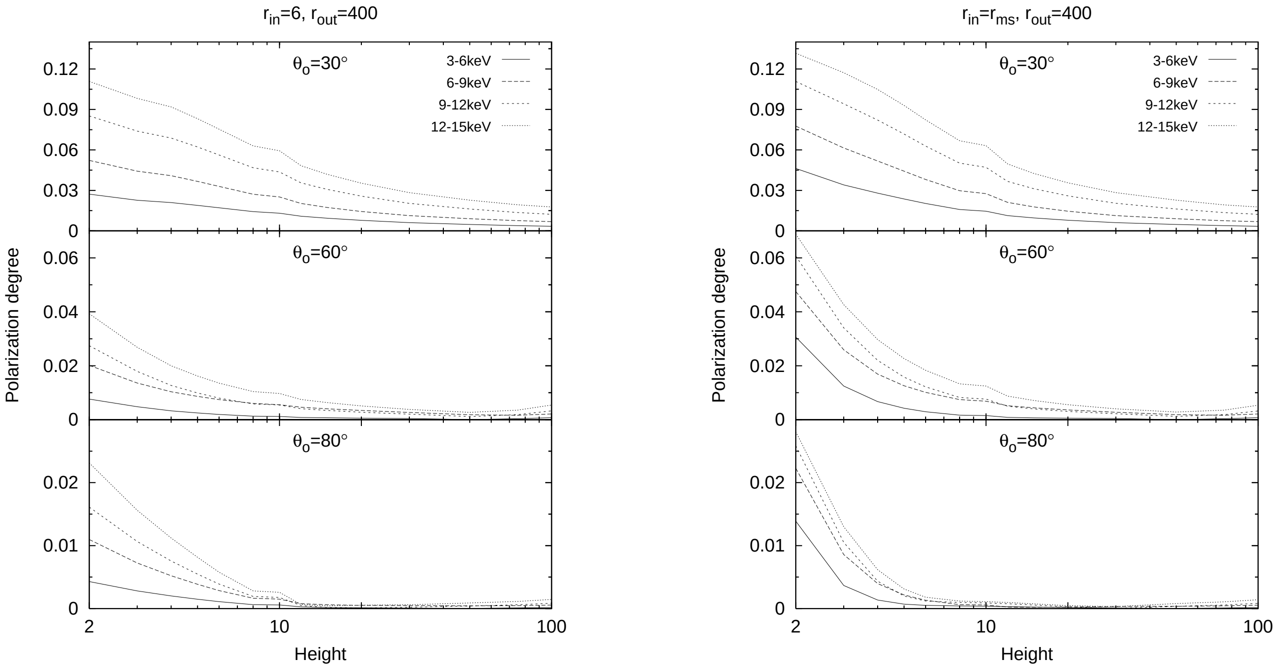

Figure 5: Net polarization degree of the total (primary plus reflected) signal as a function of h. Left panel: $r_{\rm in} = 6$; right panel: $r_{\rm in} = 1.20$. The curves are parametrized by the corresponding energy range.

the energy range of an observation. The overall degree of polarization increases with energy (see bottom panels in Figs. 1–2) due to the fact that the intensity of radiation from the primary source diminishes, the intensity of the reflected radiation increases with energy (in the energy range $3-15\,\mathrm{keV}$) and the polarization of the reflected light alone stays roughly constant.

In our computations we assumed that the irradiating source emits isotropically and its light is affected only by gravitational redshift and lensing, according to the source location at $z = h$ on axis. This results in a dilution of primary light by factor $\sim g_{\rm h}^2(h,\theta_{\rm o})\,l_{\rm h}(h,\theta_{\rm o})$, where $g_{\rm h}^2 = 1 - 2h/(a^2 + h^2)$ is square of the redshift of primary photons reaching directly the observer, $l_{\rm h}$ is the corresponding lensing factor. Here, the redshift is the dominant relativistic term, while lensing of primary photons is a few percent at most and can be safely ignored. Anisotropy of primary radiation may further attenuate or amplify the polarization degree of the final signal, while the polarization angle is almost independent of this influence as long as the primary light is itself unpolarized.

The polarization of scattered light is also shown in Fig. 3, where we plot the polarization degree and the change of the polarization angle as functions of h. Notice that in the Newtonian case only polarization angles of $0°$ or $90°$ would be expected for reasons of symmetry. The change in angle is due to gravitation for which we assumed a rapidly rotating black hole. The two panels of this figure correspond to different locations of the inner disc edge: $r_{\rm in} = 6$ and $r_{\rm in} = 1.20$, respectively. The curves are strongly sensitive to $r_{\rm in}$ and h, while the dependence on $r_{\rm out}$ is weak for a large disc (here $r_{\rm out} = 400$). Sensitivity to $r_{\rm in}$ is particularly appealing if one remembers practical difficulties in estimating $r_{\rm in}$ by fitting spectra. The effect is clearly visible even for $h \sim 20$. Graphs corresponding to $r_{\rm in} = 6$ and $a = 0.9987$ resemble the non-rotating case ($a = 0$) quite closely because dragging effects are most prominent near horizon.

Figure 4 shows the polarization degree and angle as functions of the observer's inclination. Again, by comparing the two cases of different $r_{\rm in}$ one can clearly recognize that the polarization is sensitive to details of the flow near the inner disc boundary. Finally, dependence of the polarization degree of overall radiation (primary plus reflected) on the height of the primary source and the observer inclination in different energy ranges is shown in Figures 5–6.

4. CONCLUSIONS

We examined strong-gravity polarization features in X-rays reflected from accretion discs. In order to compute directly observable characteristics one has to combine the primary continuum with the reflected component. Polarization degree of the resulting signal depends on mutual proportion of the two components and the energy range of observation. Polarization properties represent the scattering mechanism, source geometry as well as the gravitational

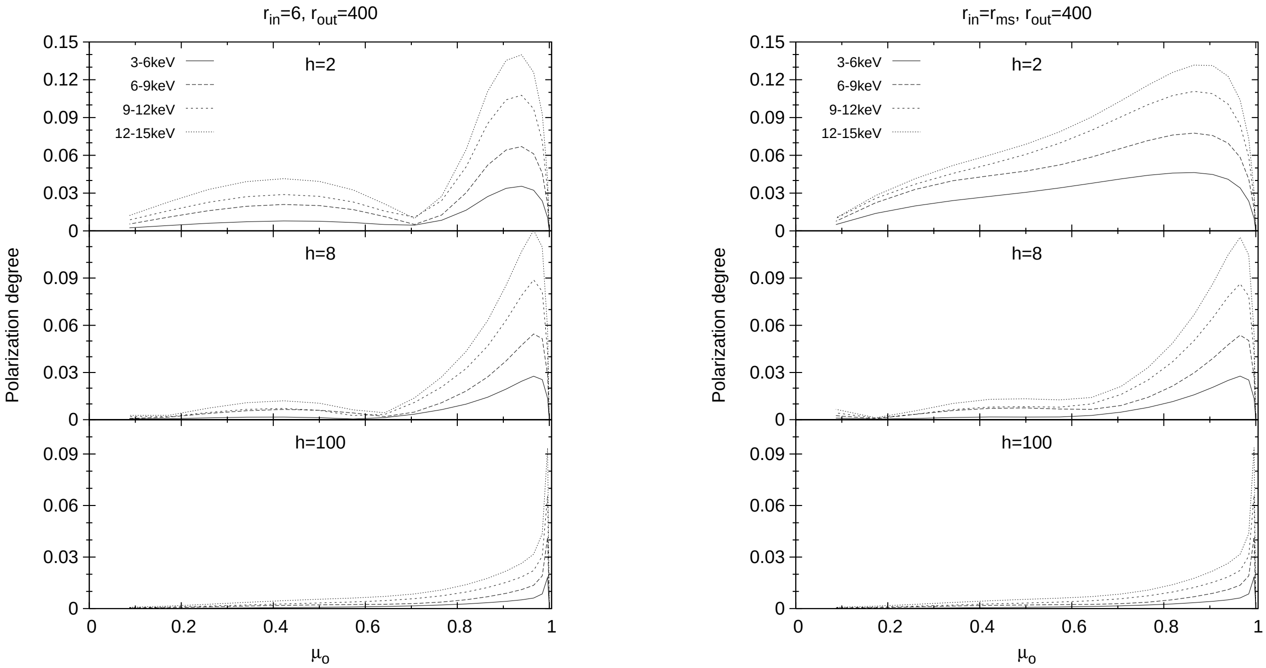

Figure 6: Net polarization degree of the total (primary plus reflected) signal as a function of μ_o. The same model is shown as in the previous figure.

field structure acting on reflected photons. New generation photoelectric polarimeters in the focal plane of large area optics, such as those foreseen for *Xeus*, can probe polarization degree of the order of one percent in bright AGN, making polarimetry, along with timing and spectroscopy, a tool for exploring the properties of the accretion flows in the vicinity of black holes.

The authors gratefully acknowledge support from Czech Science Foundation grants 205/03/0902 (VK) and 205/05/P525 (MD), and from the Grant Agency of the Academy of Sciences (IAA 300030510). GM acknowledges financial support from Agenzia Spaziale Italiana (ASI) and Ministero dell'Istruzione, dell'Università e della Ricerca (MIUR), under grant COFIN–03–02–23.

References

[1] Agol E., Blaes O., 1996, MNRAS, 282, 965

[2] Bao G., Wiita P. J., Hadrava P., 1996, PhRvL, 77, 12

[3] Bianchi S., Matt G., Balestra I., Guainazzi M., Perola G. C., 2004, A&A, 422, 65

[4] Connors P. A., Piran T., Stark R. F., 1980, ApJ, 235, 224

[5] Costa E., Soffitta P., Bellazzini R., Brez A., Lumb N., Spandre G., 2001, Nature, 411, 662

[6] Czerny B., Różańska A., Dovčiak M., Karas V., Dumont A.-M., 2004, A&A, 420, 1

[7] Dovčiak M., Bianchi S., Guainazzi M., Karas V., Matt G., 2004, MNRAS, 350, 745

[8] Dovčiak M., Karas V., Matt G., 2004, MNRAS, 355, 1005

[9] Dovčiak M., Karas V., Yaqoob T., 2004, ApJS, 153, 205

[10] Fabian A. C., Iwasawa K., Reynolds C. S., Young A. J., 2000, PASP, 112, 1145

[11] Fabian A. C. et al., 2002, MNRAS, 335, L

[12] Guainazzi M., 2003, A&A, 401, 903

[13] Laor A., Netzer H., Piran T., 1990, MNRAS, 242, 560

[14] Martocchia A., Matt G., 1996, MNRAS, 282, L53

[15] Miniutti G., Fabian A. C., Goyder R., Lasenby A. N., 2003, MNRAS, 344, L22

[16] Miniutti G., Fabian A. C., Miller J. M., 2004, MNRAS, 351, 466

[17] Petrucci P. O., Henri G., 1997, A&A, 326, 99

[18] Portsmouth J., Bertschinger E., 2004, astro-ph/0412094

[19] Pozdnyakov L. A., Sobol I. M., Sunyaev R. A., 1979, A&A, 75, 214

[20] Rees M. J., 1975, MNRAS, 171, 45

[21] Reynolds C. S., Nowak M. A., 2003, PhR, 377, 389

[22] Turner T. J. et al., 2002, ApJ, 574, L123

[23] Turner T. J., Kraemer S.B., Reeves J.N., 2004, ApJ, 603, 62

[24] Yaqoob T., George I. M., Kallman T. R., Padmanabhan U., Weaver K. A., Turner T. J., 2003, ApJ, 596, 85